

# Orthogonal Statistical Inference for Multimodal Data Analysis

XIAOWU DAI AND LEXIN LI

*University of California at Berkeley*

## Abstract

Multimodal imaging has transformed neuroscience research. While it presents unprecedented opportunities, it also imposes serious challenges. Particularly, it is difficult to combine the merits of interpretability attributed to a simple association model and flexibility achieved by a highly adaptive nonlinear model. In this article, we propose an orthogonal statistical inferential framework, built upon the Neyman orthogonality and a form of decomposition orthogonality, for multimodal data analysis. We target the setting that naturally arises in almost all multimodal studies, where there is a primary modality of interest, plus additional auxiliary modalities. We successfully establish the root- $N$ -consistency and asymptotic normality of the estimated primary parameter, the semi-parametric estimation efficiency, and the asymptotic honesty of the confidence interval of the predicted primary modality effect. Our proposal enjoys, to a good extent, both model interpretability and model flexibility. It is also considerably different from the existing statistical methods for multimodal data integration, as well as the orthogonality-based methods for high-dimensional inferences. We demonstrate the efficacy of our method through both simulations and an application to a multimodal neuroimaging study of Alzheimer’s disease.

**Key Words:** Basis expansion; High-dimensional inference; Multimodal data integration; Neuroimaging analysis; Neyman orthogonality; Reproducing kernel Hilbert space.

# 1 Introduction

Multimodal neuroimaging, where different types of images are acquired for a common set of experimental subjects, is becoming a norm in neuroscience research. It utilizes different physical and physiological sensitivities of imaging scanners and technologies, and measures distinct brain characteristics including brain structures, functions and chemical constituents. Multimodal neuroimaging analysis aggregates such diverse but often complementary information, consolidates knowledge across different modalities, and produces improved understanding of neurological development or disorders (Uludağ and Roebroek, 2014). Multimodal data also frequently arise in many other scientific applications, e.g., integrative genomics (Richardson et al., 2016), multimodal healthcare (Cai et al., 2019), and audio-visual speech recognition (Baltrusaitis et al., 2019).

Our motivation is a multimodal neuroimaging study of Alzheimer’s disease (AD). AD is an irreversible neurodegenerative disorder and the leading form of dementia in elderly subjects. The most notable AD imaging biomarker is the brain grey matter cortical atrophy measured by structural magnetic resonance imaging (MRI). Meanwhile, amyloid- $\beta$  and tau are two hallmark pathological proteins that are believed to be part of the driving mechanism of AD, and both can be measured by positron emission tomography (PET) using different nuclear tracers. The current model of AD pathogenesis hypothesizes a sequence of biological cascade among different AD biomarkers (Jack et al., 2010, 2013). It is of great scientific interest to study how they interact with each other and how they affect the cognitive outcome. These questions are crucial for our understanding of AD pathophysiology, and also have important therapeutic implications.

While multimodal neuroimaging presents unprecedented opportunities, it also imposes numerous serious challenges. First, neuroimaging data are typically high-dimensional and highly correlated, with measurements of brain characteristics at hundreds of brain regions and millions of brain voxel locations, and those measurements are often spatially or temporally correlated. Besides, the associations between different imaging modalities, and between images and phenotypic outcomes, are complicated. A linear association model, despite its wide usage, is hardly adequate to capture such complex associations. Second, it is particularly challenging to balance between model interpretability and model flexibility. Breiman (2001) contrasted two modeling cultures: the “data modeling culture”, which adopts parametric models that are easier to interpret

and to perform inference but much less flexible, versus the “algorithmic modeling culture”, also known as machine learning, which involves complex and sometimes black-box type models that are highly flexible and nonlinear but difficult to interpret and infer. Both approaches have been frequently adopted in neuroimaging analysis. Nevertheless, it is difficult to combine the merits of both. Most existing works on multimodal data integration either assume a simple parametric model for easy interpretation (e.g., Sperling et al., 2019; Li and Li, 2020), or consider a flexible nonlinear model but sacrifice the interpretability or inference capability (e.g., Hinrichs et al., 2011; Alam et al., 2018). Finally, rigorously quantifying statistical significance of the primary parameter of interest remains a fundamental question in scientific inquiries. There have been a large number of highly successful nonlinear modeling techniques, ranging from the more classical splines, reproducing kernels, and random forests, to more recent deep neural network models. However, it is notoriously difficult to carry out statistical inference when utilizing those flexible methods. Moreover, when it comes to inference, naively adding multiple modalities together may suffer from serious biases and produce misleading results, as we show later.

In this article, we propose an orthogonal statistical inferential framework, built upon the Neyman orthogonality (Neyman, 1959, 1979), and a form of decomposition orthogonality (Wahba, 1990, Chapter 3), for multimodal data analysis. The principal setting we target is that there is a *primary* modality of interest, plus additional *auxiliary* modalities. Such a setting naturally arises in almost all multimodal studies, and is particularly useful from the perspective of scientific inquiries. For instance, in AD pathophysiology modeling (Jack et al., 2013), it is often of interest to quantify the effect of brain structural atrophy on cognition after accounting for amyloid- $\beta$  and tau accumulations. In this case, the structural atrophy can be treated as the primary modality, while amyloid-beta and tau are the auxiliary modalities. In imaging genetics studies (Zhu et al., 2014; Nathoo et al., 2019), brain imaging features often play the role of intermediate phenotype between the genetic variants and clinical outcome. In this case, the brain image can be taken as the primary modality, and the genetic variants as the auxiliary modality. Under this setting, we employ a basis expansion type model along with model error to characterize the association between the primary modality and the outcome, and develop rigorous inference methods for the main parameter of interest as well as the predicted primary modality effect. Meanwhile, we employ highly flexible machine learning methods to model the complex associations both between the auxiliary modal-

ities and the outcome, and between the primary and auxiliary modalities. A key challenge that comes with flexible machine learning modeling is that its associated regularization bias and overfitting would introduce heavy bias in the estimation of the main parameter of interest. To remove such an impact, we employ two types of orthogonality formulations based on Neyman (1959, 1979) and Wahba (1990), plus cross-fitting and residual learning. We successfully establish the  $\sqrt{N}$ -consistency and asymptotic normality of the estimated main parameter, the semi-parametric estimation efficiency, as well as the asymptotic honesty of the confidence interval of the predicted primary modality effect, where  $N$  is the sample size. Our proposed framework thus enjoys, to a good extent, both model interpretability and model flexibility.

Our proposal is considerably different from the existing statistical methods for multimodal data integration. Particularly, there have been a class of unsupervised multimodal analysis built on matrix or tensor factorization (Lock et al., 2013), or canonical correlation analysis (Mai and Zhang, 2019; Shu et al., 2020). By contrast, we aim at a supervised regression problem. Under the regression setting with multimodal predictors, Li et al. (2019) proposed an integrative reduced-rank regression. Xue and Qu (2020) developed an estimating equations approach to accommodate block missing patterns. Li and Li (2020) developed a factor analysis-based linear regression model. These methods are supervised, but all of them still assume linear type associations, and none utilizes any nonlinear machine learning modeling.

Relatedly, the Neyman orthogonality has played an important role in both statistics and econometrics. Early works date back to Newey (1990); Robins and Rotnitzky (1995). Meanwhile, it has received revived interest in high-dimensional statistical inference in recent years; see Chernozhukov et al. (2018) and many references therein for a family of inference methods utilizing the Neyman orthogonality. Although our proposal is also built upon the Neyman orthogonality, there are several important differences from the existing methods. First, we extend the framework by allowing a more flexible parametric model as well as an additional model error for the primary modality. By contrast, Chernozhukov et al. (2018) focused on a low-dimensional primary parameter involving no additional error. Because of this model error, we consider another orthogonality similar to the perpendicularity in smoothing splines (Wahba, 1990), construct a new reproducing kernel Hilbert space (RKHS), and employ residual learning to remove the impact of model error in both estimation and inference. Second, we obtain the confidence band for the nonparametric

primary regression function given the high-dimensional and nonlinear nuisance functions. We show that it is asymptotically honest, by studying a Gaussian multiplier process approximation. By contrast, the existing literature on high-dimensional nonparametric inference usually requires stronger conditions that are unlikely to hold in multimodal neuroimaging data. Later, we compare with a number of existing alternative solutions both analytically and numerically.

The rest of the article is organized as follows. We introduce the model framework in Section 2, and develop an estimation procedure in Section 3. We derive the orthogonal statistical inference procedure and the theoretical guarantees in Section 4. We analytically compare with the alternative methods in Section 5. We present the simulations in Section 6, and revisit the multimodal AD study in Section 7. We relegate all proofs to the Supplementary Appendix.

## 2 Model

Suppose there are  $M + 1$  modalities of predictors. Let  $X = (X_{(1)}, \dots, X_{(p)})^\top \in \mathcal{X}^p$  denote the  $p$ -dimensional random vector of the primary modality, where  $\mathcal{X} \subset \mathbb{R}$  is a compact domain, and  $X$  follows the distribution  $P$  in the domain  $\mathcal{X}^p$ . Let  $Z_{(m)} \in \mathbb{R}^{p'_m}$  denote the  $p'_m$ -dimensional random vector of the  $m$ th auxiliary modality,  $m = 1, \dots, M$ , and let  $Z = (Z_{(1)}^\top, \dots, Z_{(M)}^\top)^\top \in \mathbb{R}^{p'}$  collect all auxiliary modalities,  $p' = p'_1 + \dots + p'_M$ . Let  $Y \in \mathbb{R}$  denote the response variable. We propose the following model framework,

$$Y = f_0(X) + g_0(Z) + U, \quad (1)$$

where  $U \in \mathbb{R}$  is the measurement error that is independent of  $(X, Z)$  and  $\mathbb{E}[U] = 0$  and  $\mathbb{E}[U^2] = \sigma^2 < \infty$ ,  $f_0$  is the regression function capturing the effect of the primary modality on the response, and  $g_0$  is the function capturing the collective effects of the auxiliary modalities. We also note that we can extend (1) from a linear model form to a generalized linear model form, so that it works for a binary or count type of response variable.

Next, assuming that  $f_0 : \mathcal{X}^p \rightarrow \mathbb{R}$  resides in an RKHS (Wahba, 1990), we decompose  $f_0$  as,

$$f_0(x) = \eta(x, \theta_0) + \delta_0(x), \quad (2)$$

where  $\eta(\cdot, \theta_0)$  is a parametric component that preserves the interpretability of  $f_0(\cdot)$ , and  $\delta_0$  is a nonparametric component that accounts for model error. Together, they form a nonparametric

model for  $f_0(x)$ . Despite the wide use of a simple linear model for  $f_0(\cdot)$  in the literature, there has been ample evidence showing that the linear model is inadequate to capture the complex association between  $X$  and  $Y$  (e.g., Alam et al., 2018). This has motivated us to consider a more flexible model for  $\eta(\cdot, \theta_0)$ , meanwhile taking into account the model error  $\delta_0(\cdot)$  as in (2).

Next, we employ a basis expansion type model for  $\eta(x, \theta_0)$ , due to its ease of interpretation, relative flexibility, as well as computational efficiency (Huang et al., 2007; Wang et al., 2014; Ma et al., 2015). Specifically, let  $\{\phi_1, \dots, \phi_s\}$  denote a collection of orthonormal and centered basis functions in  $\mathcal{X}$ , satisfying that  $\mathbb{E}[\phi_k(X_{(j)})] = 0$ ,  $j = 1, \dots, p$ ,  $k = 1, \dots, s$ , where  $s$  is the number of basis functions. There is a rich library of basis functions, including polynomial basis, Fourier basis, B-splines, among others. Denote  $\mathcal{B}_s(x_{(j)}) = \text{Span}\{1, \phi_1(x_{(j)}), \dots, \phi_s(x_{(j)})\}$  as the space spanned by these basis functions. Let the parametric component  $\eta(x, \theta_0)$  be the projection of  $f_0$  onto the space spanned by the tensor product of the basis functions, i.e.,

$$\eta(x, \theta_0) = \arg \min_{f \in \otimes_{j=1}^p \mathcal{B}_s(x_{(j)})} \int_{\mathcal{X}^p} [f(x) - f_0(x)]^2 dP(x) = \Phi(x)^\top \theta_0, \quad (3)$$

where  $x = (x_{(1)}, \dots, x_{(p)})^\top \in \mathcal{X}^p$ , the basis vector  $\Phi(x) = [1, \phi_1(x_{(1)}), \dots, \phi_s(x_{(1)}), \dots, \phi_1(x_{(p)}), \dots, \phi_s(x_{(p)}), \dots, \phi_1(x_{(1)}) \cdots \phi_p(x_{(p)})]^\top \in \mathbb{R}^d$ , and  $d = (s+1)^p$ . Model (3) is a general model that includes main effects  $\phi_i(x_{(j)})$ ,  $i = 1, \dots, s$ ,  $j = 1, \dots, p$ , pairwise interactions  $\phi_{i_1}(x_{(j_1)})\phi_{i_2}(x_{(j_2)})$ ,  $i_1, i_2 = 1, \dots, s$ ,  $j_1, j_2 = 1, \dots, p$ , as well as higher-order interactions. It includes additive model (Hastie and Tibshirani, 1990), linear model, and functional ANOVA model (Lin and Zhang, 2006) as special cases. That is, when  $\eta(x, \theta_0)$  is the projection of  $f_0$  onto the space  $\oplus_{j=1}^p \mathcal{B}_s(x_{(j)})$  spanned by the sum of the basis, then (3) is essentially an additive model. When  $s = 1$  and  $\phi_s(\cdot)$  is a centered linear basis function, (3) becomes a linear model. When  $\eta(x, \theta_0)$  is the projection of  $f_0$  onto the space spanned by the tensor product of the basis with pairwise or higher-order interactions, (3) becomes a functional ANOVA model.

Finally, we characterize the association between the primary modality  $X$  and the auxiliary modalities  $Z$  as,

$$\Phi(X) = r_0(Z) + V, \quad \mathbb{E}[V|Z] = 0, \quad (4)$$

where  $V \in \mathbb{R}^d$  accounts for the part of the variation in  $\Phi(X)$  that cannot be explained by  $Z$ , and  $r_0$  captures the complicated association between  $Z$  and  $\Phi(X)$ .

Suppose the observed data  $\{(X_i, Z_i, Y_i) : i = 1, \dots, N\}$  are independent copies of  $(X, Z, Y)$  and satisfy the system of models (1) to (4). Our main goal is the statistical inference of  $\theta_0$ ,

which reflects the interpretable effect of the primary modality  $X$  on the outcome  $Y$ , and of  $f_0$ , which reflects the predicted effect of the primary modality, and is also directly related to some causal effect and the quantification of the contribution of  $X$ . Meanwhile, we view  $\{g_0, \delta_0, r_0\}$  as nuisance functions, and propose to use highly flexible machine learning methods, e.g., random forests, reproducing kernels, or neural networks, to model them. The machine learning methods often use regularization to avoid overfitting, especially when  $X$  and  $Z$  are high-dimensional and highly nonlinear. However, regularization would introduce sizable bias, and would invalidate the subsequent inference on  $\theta_0$  and  $f_0$ . Actually, the naive estimator of  $\theta_0$  by simply plugging in the machine learning estimators of  $\{g_0, \delta_0, r_0\}$  would fail to be  $\sqrt{N}$ -consistent; see Section 5. This has motivated us to develop an orthogonal statistical inference framework to correct the bias introduced by the flexible estimators of  $\{g_0, \delta_0, r_0\}$ , and to perform a valid inference for  $\theta_0$  and  $f_0$ .

### 3 Orthogonal Estimation

We consider two orthogonality formulations that are essential for the construction of our estimator. We then present our estimation algorithm built on those orthogonal formulations.

#### 3.1 Orthogonality

The first is the Neyman orthogonality (Neyman, 1959, 1979), which allows the estimation of  $\theta_0$  to be locally insensitive to the values of nuisance functions, and thus one can plug in noisy estimates of the nuisance functions for the inference of  $\theta_0$ . Specifically, consider the target parameter  $\theta \in \mathbb{R}^d$ , and the nuisance functions  $r \in \mathcal{H}_r, g \in \mathcal{H}_g, \delta \in \mathcal{H}_\delta$ , where  $\mathcal{H}_r$  and  $\mathcal{H}_g$  are functional spaces of finite mean squared functions, and  $\mathcal{H}_\delta$  is an RKHS.

**Definition 1** (Neyman orthogonality). *A score function  $\psi(\theta, r, g, \delta)$  is said to satisfy the Neyman orthogonality (Neyman, 1959, 1979) if (i) The mean  $\mathbb{E}[\psi(\theta_0, r_0, g_0, \delta_0)] = 0$  at  $(\theta_0, r_0, g_0, \delta_0)$ ; (ii) The pathwise derivative map,  $\partial_r \{\mathbb{E}[\psi(\theta_0, r_0 + t(r - r_0), g_0 + t(g - g_0), \delta_0 + t(\delta - \delta_0))]\}$ , exists for all  $t \in [0, 1)$ , where  $r, g$  and  $\delta$  lie in a neighborhood of  $r_0 \in \mathcal{H}_r, g_0 \in \mathcal{H}_g$  and  $\delta_0 \in \mathcal{H}_\delta$ , respectively; (iii) The pathwise derivative vanishes at  $t = 0$ , in that  $\partial_t \{\mathbb{E}[\psi(\theta_0, r_0 + t(r - r_0), g_0 + t(g - g_0), \delta_0 + t(\delta - \delta_0))]\}|_{t=0} = 0$ .*

**Proposition 1.** *Define the score function,*

$$\psi(W; \theta, r, g, \delta) = [Y - \Phi(X)^\top \theta - g(Z) - \delta(X)][r(Z) - \Phi(X)],$$

where  $W = (X, Y, Z)$ . Then under the system of models (1) to (4), the score  $\psi(W; \theta, m, \delta, g)$  is Neyman orthogonal at  $(\theta_0, r_0, g_0, \delta_0)$ .

In addition to the Neyman orthogonality, we also require that the functions  $\Phi$  and  $\delta_0$  in models (2) and (3) to satisfy a decomposition orthogonality, which is necessary for the identifiability of  $\theta_0$ . We then construct an RKHS  $\mathcal{H}_\delta$  that satisfies such an orthogonality.

**Definition 2** (Decomposition orthogonality). *Suppose that  $\Phi(\cdot)$  is bounded on  $\mathcal{X}^p$ . The functions  $\Phi$  and  $\delta_0$  are said to satisfy the decomposition orthogonality if  $\mathbb{E}_X[\Phi(X)\delta_0(X)] = 0$ .*

**Proposition 2.** *Under models (2) and (3),  $\theta_0$  is identifiable only if  $\Phi$  and  $\delta_0$  satisfy the decomposition orthogonality. Moreover, for any reproducing kernel  $K(\cdot, \cdot)$  on  $\mathcal{X}^p \times \mathcal{X}^p$ , define*

$$K_\delta(x, x') = K(x, x') - \mathbb{E}_X[\Phi(X)^\top K(x, X)] \\ \times (\mathbb{E}_X\{\mathbb{E}_{X'}[\Phi(X')K(X', X)]\Phi(X)^\top\})^{-1} \mathbb{E}_{X'}[\Phi(X')K(x', X')],$$

where  $X$  and  $X'$  are i.i.d. copies of the primary modality. Then  $K_\delta(\cdot, \cdot) : \mathcal{X}^p \times \mathcal{X}^p \rightarrow \mathbb{R}$  is positive definite. Besides, for any  $\hat{\delta}(x) = \sum_{i=1}^m c_i K_\delta(x, x_i)$ , with  $c_i \in \mathbb{R}$ ,  $x_i \in \mathcal{X}^p$  and  $m \geq 1$ ,  $\Phi(X)$  and  $\hat{\delta}(X)$  satisfy the decomposition orthogonality.

The decomposition orthogonality in Definition 2 is similar to the perpendicularity requirement in the smoothing splines literature (see, e.g., Wahba, 1990, Chapter 3), where the null space and the RKHS need to be perpendicular under certain norms in order to find a consistent estimator as the sample size diverges, while we use an  $\ell_2$ -norm with respect to the distribution of  $X$ . Hereinafter, let  $\mathcal{H}_\delta$  be the corresponding RKHS of the kernel  $K_\delta(\cdot, \cdot)$ . By the representer theorem (Wahba, 1990), the  $M$ -estimator in RKHS  $\mathcal{H}_\delta$  can be found in a finite-dimensional subspace of  $\mathcal{H}_\delta$ , i.e., it can be written as  $\hat{\delta}(x) = \sum_{i=1}^m c_i K_\delta(x, x_i)$ , with  $c_i \in \mathbb{R}$ ,  $x_i \in \mathcal{X}^p$  and  $m \geq 1$ . Proposition 2 shows that  $\hat{\delta}(X)$  and  $\Phi(X)$  satisfy the decomposition orthogonality, which in turn ensures the identifiability of the primary parameter  $\theta_0$  we target.

### 3.2 Iterative cross-fitting procedure

We next present an estimation algorithm of  $\theta_0$  based on the orthogonality formulations in Propositions 1 and 2. The algorithm consists of five main steps. In the first step, we obtain the initial



---

**Algorithm 1** Orthogonal estimation algorithm

---

- 1: Obtain the initial estimators  $\widehat{\theta}^{(0)}, \widehat{g}^{(0)}, \widehat{\delta}^{(0)}$  by (5) using all the data.
  - 2: Split the data randomly into  $Q$  non-overlapping chunks of equal size. For  $q \in [Q]$ , denote  $I_q$  as the corresponding set of data indices of the  $q$ th chunk, and  $I_q^c = [N] \setminus I_q$ .
  - 3: **for**  $q = 1$  to  $Q$  **do**
  - 4:   Obtain the estimator  $\widehat{r}_0$  by (6) using the data in  $I_q^c$ .
  - 5: **end for**
  - 6: **repeat**
  - 7:   **for**  $q = 1$  to  $Q$  **do**
  - 8:     Obtain the iterative estimators  $\{\widehat{g}_q^{(t)}, \widehat{\delta}_q^{(t)}\}$  by (7) using the data in  $I_q^c$ .
  - 9:     Obtain the iterative estimator  $\widehat{\theta}_q^{(t)}$  by (8) using the data in  $I_q$ .
  - 10:   **end for**
  - 11:   Obtain the iterative estimator  $\widehat{\theta}^{(t)}$  by (9).
  - 12: **until** the stopping criterion is met.
  - 13: Construct the final estimator  $\widehat{\theta} \in \mathbb{R}^d$  by (10) using cross-fitting.
- 

estimators of  $\{\theta_0, g_0, \delta_0\}$ . In the second step, we split the data into  $Q$  disjoint chunks. In the third step, we estimate  $r_0$ , and in the fourth step, we iteratively update the estimates of  $\{g_0, \delta_0\}$  and  $\theta_0$ . In these two steps, we obtain the estimates by leaving out some chunk of data in turn. In the fifth step, we construct the final estimator of  $\theta_0$ , by first using only one chunk of data at a time, then averaging over all  $Q$  chunks. When estimating the nuisance functions  $\{r_0, g_0, \delta_0\}$ , we employ some penalized learning methods, where we denote  $\text{PEN}_{\mathcal{H}_r}(r)$ ,  $\text{PEN}_{\mathcal{H}_g}(g)$ ,  $\text{PEN}_{\mathcal{H}_\delta}(\delta)$  as the penalty functionals in the candidate functional spaces  $\mathcal{H}_r$ ,  $\mathcal{H}_g$ ,  $\mathcal{H}_\delta$ , respectively. Here,  $\mathcal{H}_\delta$  is chosen to be the corresponding RKHS of  $K_\delta(\cdot, \cdot)$  in Proposition 2, and  $\text{PEN}_{\mathcal{H}_\delta}(\delta)$  is the penalty based on the squared RKHS-norm in  $\mathcal{H}_\delta$ . The choices of  $\{\mathcal{H}_r, \mathcal{H}_g\}$  as well as the penalty functions depend on specific data applications, and the tuning follows the usual tuning procedures in penalized learning. We first summarize the procedure in Algorithm 1, then detail the main steps.

In the first step, we obtain the initial estimators of  $\{\theta_0, g_0, \delta_0\}$  as,

$$\begin{aligned}\widehat{\theta}^{(0)} &= \arg \min_{\theta \in \mathbb{R}^d} \left\{ \frac{1}{N} \sum_{i=1}^N [Y_i - \Phi(X_i)^\top \theta - \widehat{g}^{(0)}(Z)]^2 \right\}, \\ \widehat{g}^{(0)} &= \arg \min_{g \in \mathcal{H}_g} \left\{ \frac{1}{N} \sum_{i=1}^N [Y_i - g(Z_i)]^2 + \lambda_N^g \text{PEN}_{\mathcal{H}_g}(g) \right\},\end{aligned}\tag{5}$$

and  $\widehat{\delta}^{(0)} = 0$ . Here,  $\lambda_N^g \geq 0$  is a tuning parameter, and we use all the  $N$  data samples.

In the second step, we randomly split the sample observations into  $Q \geq 2$  non-overlapping

chunks of equal size  $n = N/Q$ . For notational simplicity, we assume  $N$  is divisible by  $Q$ . For each  $q \in [Q] = \{1, \dots, Q\}$ , we denote  $I_q$  as the set of indices in  $[N] = \{1, \dots, N\}$  corresponding to the data in the  $q$ th chunk, and denote  $I_q^c = [N] \setminus I_q$  as the indices of the complementary data.

In the third step, we estimate the function  $r_0$  by,

$$\hat{r}_q = \arg \min_{r \in \mathcal{H}_r} \left\{ \frac{1}{n} \sum_{i \in I_q^c} [\Phi(X_i) - r(Z_i)]^2 + \lambda_n^r \text{PEN}_{\mathcal{H}_r}(r) \right\}, \quad (6)$$

where  $\lambda_n^r \geq 0$  is a tuning parameter. Note that we only utilize the data from  $I_q^c$  in (6). Besides, we estimate  $r_0$  only once, without any iterations, for each  $q \in [Q]$ .

In the fourth step, we iteratively update the estimates of  $\{g_0, \delta_0\}$  and  $\theta_0$ . That is,

$$\begin{aligned} \left\{ \hat{g}_q^{(t)}, \hat{\delta}_q^{(t)} \right\} = & \arg \min_{g \in \mathcal{H}_g, \delta \in \mathcal{H}_\delta} \left\{ \frac{1}{n} \sum_{i \in I_q^c} \left[ Y_i - \Phi(X_i) \hat{\theta}^{(t-1)} - \delta(X_i) - g(Z_i) \right]^2 \right. \\ & \left. + \lambda_n^g \text{PEN}_{\mathcal{H}_g}(g) + \lambda_n^\delta \text{PEN}_{\mathcal{H}_\delta}(\delta) \right\}, \end{aligned} \quad (7)$$

$$\begin{aligned} \tilde{\theta}_q^{(t)} = & \left\{ \frac{1}{n} \sum_{i \in I_q} [\Phi(X_i) - \hat{r}_q(Z_i)] \Phi(X_i)^\top \right\}^{-1} \\ & \times \frac{1}{n} \sum_{i \in I_q} [\Phi(X_i) - \hat{r}_q(Z_i)] \left[ Y_i - \hat{g}_q^{(t)}(Z_i) - \hat{\delta}_q^{(t)}(X_i) \right], \end{aligned} \quad (8)$$

$$\hat{\theta}^{(t)} = \frac{1}{Q} \sum_{q=1}^Q \tilde{\theta}_q^{(t)}, \quad (9)$$

where  $\lambda_n^g, \lambda_n^\delta \geq 0$  are the tuning parameters. The estimation in (7) employs residual learning, since it is based on the residual  $[Y - \Phi(X) \hat{\theta}_q^{(t-1)}]$ . The resulting estimator  $\hat{\delta}_q^{(t)}$  satisfies the decomposition orthogonality relative to  $\Phi$  in Proposition 2. Besides, it involves only the complementary data in  $I_q^c$ . The estimation in (8) employs the Neyman orthogonality formulation in Proposition 1, and involves only the data in  $I_q$ . The estimation in (9) averages  $\tilde{\theta}_q^{(t)}$  from (8) across all  $q = 1, \dots, Q$ . Moreover, (8) and (9) together utilize the idea of centralized training with decentralized execution (Lowe et al., 2017), which greatly facilitates the convergence of the algorithm. We stop the iterations when some stopping criterion is met, e.g., when the difference between two consecutive estimates of  $\theta_0$  is smaller than a threshold value. We also remark that, this step is essentially a Gauss-Seidel iterative algorithm that has been widely used in statistics (Buja et al.,

1989). In our simulations, we find the algorithm converges fast, usually after only 3 to 5 iterations. We denote the final estimators for  $\{g_0, \delta_0\}$  as  $\{\hat{g}_q, \hat{\delta}_q\}$ ,  $q \in [Q]$ .

In the final step, we construct the orthogonal estimator for  $\theta_0$  using cross-fitting,

$$\begin{aligned} \hat{\theta} = & \left\{ \frac{1}{Q} \sum_{q=1}^Q \frac{1}{n} \sum_{i \in I_q} [\Phi(X_i) - \hat{r}_q(Z_i)] \Phi(X_i)^\top \right\}^{-1} \\ & \times \frac{1}{Q} \sum_{q=1}^Q \frac{1}{n} \sum_{i \in I_q} [\Phi(X_i) - \hat{r}_q(Z_i)] \left[ Y_i - \hat{g}_q(Z_i) - \hat{\delta}_q(X_i) \right]. \end{aligned} \quad (10)$$

That is, for each  $q \in [Q]$ , we use the chunk of data that is left out when estimating  $\{r_0, g_0, \delta_0\}$  earlier, then average over all  $Q$  chunks. Cross-fitting has been commonly used in high-dimensional inferences in recent years; see, e.g., Chernozhukov et al. (2018); Newey and Robins (2018). By swapping the roles of each chunk and the complementary chunks  $Q$  times, it ensures good statistical properties while regaining the efficiency of making use of all available data observations. Later, we show the estimator  $\hat{\theta}$  in (10) is actually semi-parametric efficient.

## 4 Orthogonal Statistical Inference

For orthogonal statistical inference, we aim at two key questions: inference for the primary parameter of interest  $\theta_0$ , and inference for the primary regression function  $f_0(\cdot)$ . Both are crucial for scientific inquiries. The former directly quantifies the relevance of the variables of the primary modality to the outcome. The latter captures the predicted effect and the contribution of the primary modality, and also has some causal interpretation under additional conditions.

### 4.1 Inference of the primary parameter $\theta_0$

We begin with the study of the asymptotic behavior of the estimator  $\hat{\theta}$  in (10) as the sample size  $N$  tends to infinity. We establish the  $\sqrt{N}$ -convergence that  $\|\hat{\theta} - \theta_0\|_{\ell_2} = O_p(N^{-1/2})$ , as well as the asymptotic normality that  $\sqrt{N}(\hat{\theta} - \theta_0)$  approaches a normal distribution. We note that this  $\sqrt{N}$ -convergence result is highly nontrivial, because the estimator  $\hat{\theta}$  in (10) involves the nuisance estimators  $\{\hat{r}_q, \hat{g}_q, \hat{\delta}_q\}$ . When  $\{r_0, g_0, \delta_0\}$  are estimated nonparametrically, the convergence rates of the estimators  $\{\hat{r}_q, \hat{g}_q, \hat{\delta}_q\}$  are generally slower than  $O_p(N^{-1/2})$  (van der Vaart, 1998). Later in Section 5, we show that many popular alternative methods cannot achieve the  $\sqrt{N}$ -consistency.

We first present a set of regularity conditions.

- (C1) The basis vector  $\Phi(\cdot)$  in (3) satisfies that  $\mathbb{E}[\|\Phi(X)\|_{\ell_2}^2] < \infty$ .
- (C2) The error term  $V \in \mathbb{R}^d$  in (4) satisfies that  $\mathbb{E}(VV^\top)$  is invertible and  $\mathbb{E}(V^\top V) < \infty$ .
- (C3) The estimators  $\hat{r}_q$  as constructed in (6), and  $\{\hat{g}_q, \hat{\delta}_q\}$  as constructed in (7) at the algorithmic convergence satisfy that  $\mathbb{E}[\|\hat{r}_q(Z) - r_0(Z)\|_{\ell_2}^2] = o(N^{-1/2})$ ,  $\mathbb{E}\{[\hat{g}_q(Z) - g_0(Z)]^2\} = o(N^{-1/2})$ , and  $\mathbb{E}\{[\hat{\delta}_q(X) - \delta_0(X)]^2\} = o(N^{-1/2})$ , for  $q \in [Q]$  and  $Q$  is finite.

Condition (C1) is mild and holds for most practical choices of the basis functions. For example, (C1) holds with the continuous basis over the compact domain  $\mathcal{X}^p$ . Condition (C2) is a fairly standard regularity condition, and is needed for the asymptotic normality of parameter estimation in moment-based problems (Chernozhukov et al., 2018). Condition (C3) is different from requiring the estimators  $\{\hat{r}_q, \hat{g}_q, \hat{\delta}_q\}$  to be  $\sqrt{N}$ -consistent, which is difficult to satisfy for many nonparametric estimators. Instead, (C3) holds for a wide range of popular machine learning methods; for instance, it holds for the  $\ell_1$ -penalized linear regression in a variety of sparse models (Bickel et al., 2009; Bühlmann and van de Geer, 2011), a class of random forests (Biau, 2012), a class of neural networks (Chen and White, 1999), and numerous kernel methods in RKHS (Wahba, 1990; van der Vaart, 1998), among others. Moreover, we note that (C3) is generally less restrictive than the Donsker conditions, which are commonly assumed in semi-parametric statistical analysis (Kosorok, 2007). The Donsker conditions require the functional spaces  $\{\mathcal{H}_r, \mathcal{H}_g, \mathcal{H}_\delta\}$  to have a bounded complexity, or more specifically, a bounded entropy integral. However, for multimodal data analysis where the dimension of the auxiliary modalities  $Z$  increases with the sample size, such a requirement fails even in the linear model setting with the parameter space specified by the Euclidean ball of unit radius (Raskutti et al., 2011). By contrast, (C3) holds in this example.

Under (C1) to (C3), we obtain the main theoretical result of the orthogonal estimator  $\hat{\theta}$ .

**Theorem 1.** *Suppose the system of models (1) to (4), and the regularity conditions (C1) to (C3) hold. The orthogonal estimator  $\hat{\theta}$  as constructed in (10) satisfies that,*

$$\hat{\theta} - \theta_0 = [\mathbb{E}(VV^\top)]^{-1} \left( \frac{1}{N} \sum_{i=1}^N V_i U_i \right) + o_p(N^{-1/2}).$$

where  $\{(U_i, V_i) : i = 1, \dots, N\}$  are independent copies of the error terms  $(U, V)$  in (1) and (4).

The proof of this theorem is given in Supplementary Appendix. We make two remarks. First, a direct implication of Theorem 1 is the asymptotic normality of the orthogonal estimator  $\hat{\theta}$ , i.e.,

$$\sqrt{N}(\hat{\theta} - \theta_0) \xrightarrow{d} \mathcal{N}(0, \sigma^2 [\mathbb{E}(VV^\top)]^{-1}). \quad (11)$$

Second, the asymptotic normality in (11) implies that we can construct the confidence interval for the primary parameter of interest  $\theta_0$  as,

$$\text{CI}(\theta_0) = \hat{\theta} \pm F_{\mathcal{N}}^{-1}(1 - \alpha/2) \sqrt{\sigma^2 (\mathbb{E}[VV^\top])^{-1}/N},$$

where  $F_{\mathcal{N}}(\cdot)$  denotes the cumulative distribution function of the standard normal distribution.

When the variance term  $\sigma^2 \mathbb{E}[VV^\top]$  in (11) is unknown, we use a plug-in estimator,

$$\hat{\Sigma}(\hat{\theta}) = \hat{J}^{-1} \left\{ \frac{1}{nQ} \sum_{q=1}^Q \sum_{i \in I_q} \left[ Y_i - \Phi(X_i)^\top \hat{\theta} - \hat{g}_q(Z_i) - \hat{\delta}_q(X_i) \right]^2 [\hat{r}_q(Z_i) - \Phi(X_i)] [\hat{r}_q(Z_i) - \Phi(X_i)]^\top \right\} \hat{J}^{-1},$$

where  $\hat{J} = (nQ)^{-1} \sum_{q=1}^Q \sum_{i \in I_q} [\Phi(X_i) - \hat{r}_q(Z_i)] \Phi(X_i)^\top$ . The next corollary shows that this plug-in estimator is consistent, and its proof is given in Supplementary Appendix.

**Corollary 1.** *Suppose the conditions of Theorem 1 hold. If  $U$  in (1) and the elements of  $V$  in (4) have bounded fourth moment, then the plug-in estimator  $\hat{\Sigma}(\hat{\theta})$  is consistent, in that*

$$\hat{\Sigma}(\hat{\theta}) \xrightarrow{p} \sigma^2 (\mathbb{E}[VV^\top])^{-1}.$$

Next, we discuss the efficiency of the orthogonal estimator  $\hat{\theta}$  in (10). We first note that the estimation problem for  $\theta_0$  under the system of models (1) to (4) is semi-parametric. This is because the parameter of interest  $\theta_0 \in \mathbb{R}^d$  is finite-dimensional as specified in (3), while the parameter space of models (1) and (2) contains high-dimensional, or infinite-dimensional functional spaces as  $\{g_0, \delta_0\} \in \mathcal{H}_g \otimes \mathcal{H}_\delta$ . We also allow the dimensions of  $g_0$  and  $\delta_0$  to grow with the sample size  $N$ . The next theorem shows that the orthogonal estimator  $\hat{\theta}$  in (10) is semi-parametric efficient (Kosorok, 2007), in that it achieves the highest possible efficiency, if the measurement error  $U$  follows a normal distribution. The proof of this theorem is given in Supplementary Appendix, along with a brief review of the background on semi-parametric estimation efficiency.

**Theorem 2.** *Suppose the conditions of Theorem 1 hold. If the measurement error  $U$  in (1) follows a normal distribution, then the orthogonal estimator  $\hat{\theta}$  in (10) is semi-parametric efficient.*

## 4.2 Inference of the primary function $f_0$

We next study the asymptotic behavior of the primary regression function  $f_0(\cdot)$ . This is of particular interest for several reasons. First of all, it quantifies the predicted effect of the primary modality  $X$  on the outcome  $Y$ . In addition, it also captures the amount of contribution of the primary modality, in terms of the percentage of variation explained, given all other modalities in the model. Finally, under some additional assumptions,  $f_0$  is directly related to the notions of the partial dependence of  $Y$  on  $X$ , as well as the total effect of  $X$  on  $Y$  in a causal inference sense.

Given the orthogonal estimator  $\hat{\theta}$  in (10), a natural estimator for  $f_0$  is  $\hat{f}(x) = \Phi(x)^\top \hat{\theta}$ . We seek the confidence interval for  $f_0(x)$ , by considering the empirical process  $\sup_{x \in \mathcal{X}^p} \sqrt{N}[\hat{f}(x) - f_0(x)]$ , whose distribution can be approximated by a Gaussian multiplier process,

$$\hat{\mathbb{H}}_N(x) = \sqrt{N} \Phi(x)^\top \left\{ \frac{1}{nQ} \sum_{q=1}^Q \sum_{i \in I_q} [\Phi(X_i) - \hat{r}_q(Z_i)] \Phi(X_i)^\top \right\}^{-1} \frac{1}{nQ} \sum_{q=1}^Q \sum_{i \in I_q} [\Phi(X_i) - \hat{r}_q(Z_i)] \hat{\sigma}(\hat{\theta}) \xi_i,$$

where the estimator  $\hat{\sigma}^2(\hat{\theta}) = (nQ)^{-1} \sum_{q=1}^Q \sum_{i \in I_q} [Y_i - \Phi(X_i)^\top \hat{\theta} - \hat{g}_q(Z_i) - \hat{\delta}_q(X_i)]^2$ , and  $\xi = (\xi_1, \dots, \xi_N)^\top \in \mathbb{R}^N$  are independent  $\mathcal{N}(0, 1)$  random variables. Let  $\hat{c}_N(\alpha/2)$  be the  $(1 - \alpha/2)$ th quantile of  $\sup_{x \in \mathcal{X}^p} \hat{\mathbb{H}}_N(x)$ . We construct the  $100 \times (1 - \alpha)\%$  confidence interval for  $f_0(x)$  as,

$$\text{CI}(f_0(x)) = \hat{f}(x) \pm \frac{\hat{c}_N(\alpha/2)}{\sqrt{N}}, \quad x \in \mathcal{X}^p. \quad (12)$$

To establish the asymptotic validity of (12), we first present a modified version of the regularity condition (C3), and an additional condition regarding the function  $f_0$ .

(C3') The estimators  $\hat{r}_q$  as constructed in (6), and  $\{\hat{g}_q, \hat{\delta}_q\}$  as constructed in (7) at the algorithmic convergence satisfy that  $\mathbb{E}[\|\hat{r}_q(Z) - r_0(Z)\|_{\ell_2}^2] = O(N^{-1/2-c_r})$ ,  $\mathbb{E}[(\hat{g}_q(Z) - g_0(Z))^2] = O(N^{-1/2-c_g})$ , and  $\mathbb{E}[(\hat{\delta}_q(X) - \delta_0(X))^2] = O(N^{-1/2-c_\delta})$ , for some constants  $c_r, c_g, c_\delta \in (0, 1/2]$ ,  $q \in [Q]$ , and  $Q$  is finite.

(C4) The function  $f_0 : \mathcal{X}^p \rightarrow \mathbb{R}$  resides in the  $k$ th-order Sobolev space,  $k > p$ , in that  $f_0$  and the derivatives  $f_0^{(\nu)}$  are absolutely continuous for any vector of nonnegative integers  $\nu \in \mathbb{N}_0^p$  with  $\|\nu\|_{\ell_1} \leq k - 1$ , and  $\mathbb{E}\{[f_0^{(\nu)}(X)]^2\} < \infty$  for any  $\nu \in \mathbb{N}_0^p$  with  $\|\nu\|_{\ell_1} = k$ .

Condition (C3') is slightly stronger than (C3), which is necessary to obtain the uniform coverage of the confidence interval  $\text{CI}(f_0(x))$ . Nevertheless, (C3') continues to hold for a wide range

of commonly-used machine learning methods, including all the aforementioned ones where (C3) holds. Condition (C4) is a standard regularity condition in the literature on nonparametric estimations (Wahba, 1990; van der Vaart, 1998).

The next theorem shows that the confidence interval  $\text{CI}(f_0(x))$  in (12) is asymptotically honest in the sense of uniform validity (Chernozhukov et al., 2014), i.e.,

$$\liminf_{N \rightarrow \infty} \mathbb{P}[f_0(x) \in \text{CI}(f_0(x)), \text{ for all } x \in \mathcal{X}^p] \geq 1 - \alpha.$$

**Theorem 3.** *Suppose the system of models (1) to (4), and the regularity conditions (C1), (C2), (C3') and (C4) hold. Let  $s$  denote the number of bases for each function component in (3), and  $c_{\min} = \min\{c_r, c_g, c_\delta\} > 0$ . Suppose the measurement error  $U$  in (1) follows a normal distribution, and the number of basis functions  $s = \lceil N^{(1+2c)/2k} \rceil$  for a constant  $c \in (0, (k-p)/2(k+p)]$ . Then, there exist a constant  $C > 0$ , such that the coverage probability of  $\text{CI}(f_0(x))$  satisfies,*

$$\mathbb{P}[f_0(x) \in \text{CI}(f_0(x)), \text{ for all } x \in \mathcal{X}^p] \geq 1 - \alpha - CN^{-c}, \text{ for any } 0 < \alpha < 1.$$

*Consequently, the confidence interval  $\text{CI}(f_0(x))$  is asymptotic honest.*

The proof of this theorem is given in Supplementary Appendix, and is built upon the framework of using the Gaussian multiplier bootstrap to approximate the distribution of the supreme of empirical processes (Chernozhukov et al., 2014). We also remark the conditions that Theorem 3 relies on are weaker than the ones in Lu et al. (2020) and Kozbur (2020), who studied the inference for the nonparametric function  $f_0$  in the presence of potentially high-dimensional conditioning variables  $Z$ . Specifically, Lu et al. (2020) required that there only exists a weak dependency between the covariates, e.g., between  $X$  and  $Z$ , in that the difference between the joint distribution and the product of marginal distributions is small under a certain norm. Kozbur (2020) assumed that the nuisance function  $g_0$  in (1) can be well approximated using only a small number of basis functions. Multimodal data, however, are typically highly correlated, and the dependency between  $X$  and  $Z$  can be complex (Uludağ and Roebroek, 2014). As such, the requirements of Lu et al. (2020) and Kozbur (2020) may not always hold. Besides, the method of Kozbur (2020) cannot be directly used to construct a uniformly valid confidence band. By contrast, we allow a strong dependency between  $X$  and  $Z$ , where the function  $r_0$  in (4) characterizes a potentially complex dependency between different modalities. Our confidence interval in (12) is asymptotically honest under high-dimensional, highly correlated and complex dependency structures.

In addition to the predicted effect, the function  $f_0$  also captures the amount of contribution of the primary modality given other modalities. Recall that in the classical linear regression model, the coefficient of determination  $R^2$  measures the percentage of total variation in the response that has been explained by the predictors. We next show that  $f_0$  is directly related to  $R^2$ , then derive the confidence interval for the  $R^2$  measure. Consider the population version of  $R^2$ ,

$$R^2 = 1 - \frac{\mathbb{E}(\text{RSS})}{\mathbb{E}(\text{TSS})}, \quad \text{where } \mathbb{E}(\text{RSS}) = \mathbb{E}[\{Y - f_0(X)\}^2], \quad \mathbb{E}(\text{TSS}) = \mathbb{E}[(Y - \bar{Y})^2], \quad (13)$$

$\bar{Y} = N^{-1} \sum_{i=1}^N Y_i$ , and RSS and TSS denote the residual sum of squares and total sum of squares, respectively. Define  $\hat{f}_{(1)}(x) = \hat{f}(x) - N^{-1/2} \hat{c}_N(\alpha/2)$ , and  $\hat{f}_{(2)}(x) = \hat{f}(x) + N^{-1/2} \hat{c}_N(\alpha/2)$ . Then denote  $R_{(1)}^2 = 1 - \sum_{i=1}^N [Y_i - \hat{f}_{(1)}(X_i)]^2 / \sum_{i=1}^N (Y_i - \bar{Y})^2$ , and  $R_{(2)}^2 = 1 - \sum_{i=1}^N [Y_i - \hat{f}_{(2)}(X_i)]^2 / \sum_{i=1}^N (Y_i - \bar{Y})^2$ . We construct the  $100 \times (1 - \alpha)\%$  confidence interval for  $R^2$  as,

$$\text{CI}(R^2) = (\min(R_{(1)}^2, R_{(2)}^2), \max(R_{(1)}^2, R_{(2)}^2)).$$

The next corollary shows that this is a valid confidence interval. It is a direct consequence of Theorem 3, and its proof is omitted.

**Corollary 2.** *Suppose the conditions of Theorem 3 hold. The confidence interval  $\text{CI}(R^2)$  is valid, in that  $\liminf_{N \rightarrow \infty} \mathbb{P}[R^2 \in \text{CI}(R^2)] \geq 1 - \alpha$ .*

Finally, we note that  $f_0$ , under some additional conditions, has a causal interpretation, and is directly related to the notions of partial dependence and total effect. Consequently, our proposed orthogonal inference procedure for  $f_0$  may be useful for inferring causal effect.

Specifically, following Friedman (2001), the partial dependence of the response  $Y$  on the primary modality  $X = x_0 \in \mathcal{X}^p$  is defined as,

$$\mathbb{E}_Z[\mathbb{E}_U(Y)] = \mathbb{E}_Z[f_0(x_0) + g_0(z)] = f_0(x_0) + c, \quad c \in \mathbb{R}, \quad (14)$$

where  $(X, Z, Y)$  follows model (1). That is, the partial dependence is the expectation of  $Y$  over the marginal distribution of all modalities other than  $X$ . It is different from the conditional expectation,  $\mathbb{E}_Z[\mathbb{E}_U(Y)|X = x_0] = \mathbb{E}_{Z|X=x_0}[f_0(x_0) + g_0(z)]$ , where the expectation is taken over the conditional distribution of  $Z$  given  $X = x_0$ . By (14), we see that the partial dependence is equal to  $f_0(x_0)$  up to an additive constant  $c$ . This property does not hold for the conditional expectation.



Next, following Pearl (2009) and Zhao and Hastie (2021), the partial dependence measure in (14) coincides with the back-door adjustment formula for identifying the causal effect of  $X$  on  $Y$  given the observational data. More specifically, view model (1) as a structural equation model, where each of the  $(M + 1)$  modalities  $\{X, Z_{(1)}, \dots, Z_{(M)}\}$  corresponds to one of the  $(M + 1)$  nodes in a directed acyclic graph (Pearl, 2009). Let a path be a consecutive sequence of edges of the directed graph, and a back-door path be a path that contains an arrow into  $X$ . If the following back-door criteria are satisfied, such that none of  $\{Z_{(1)}, \dots, Z_{(M)}\}$  is a descendant of  $X$ , and  $\{Z_{(1)}, \dots, Z_{(M)}\}$  blocks all back-door paths between  $X$  and  $Y$ , then the partial dependence measure in (14), or equivalently  $f_0(\cdot)$ , can be interpreted as the total effect of the primary modality  $X$  affecting the outcome  $Y$ .

## 5 Comparison with Alternative Methods

We next analytically compare our method with a number of important alternative solutions, and carefully evaluate the asymptotic behavior of each estimator.

### 5.1 Unimodal regression

A common solution in practice is to focus on a single data modality and exclude all other modalities from the analysis. This approach is simple, and shares a similar spirit as the marginal regression (Fan and Lv, 2008). We term it as the *unimodal regression*. Specifically, it regresses the outcome on the primary modality, and estimate the primary parameter  $\theta_0$  by,

$$\hat{\theta}_{UR} = \arg \min_{\theta \in \mathbb{R}^d} \left\{ \frac{1}{N} \sum_{i=1}^N [Y_i - \Phi(X_i)^\top \theta]^2 \right\}.$$

Proposition 3 characterizes the asymptotic behavior of the unimodal estimator  $\hat{\theta}_{UR}$ .

**Proposition 3.** *Suppose the system of models (1) to (4) hold. Suppose  $\mathbb{E}[\Phi(X)\Phi(X)^\top]$  is invertible. Then the unimodal regression estimator  $\hat{\theta}_{UR}$  satisfies that,*

$$\hat{\theta}_{UR} - \theta_0 = \{\mathbb{E}[\Phi(X)\Phi(X)^\top]\}^{-1} \left\{ \frac{1}{N} \sum_{i=1}^N \Phi(X_i) [\delta_0(X_i) + g_0(Z_i) + U_i] \right\} + o_p(N^{-1/2}).$$

The proof of the proposition is given in Supplementary Appendix. We next compare the behavior of  $\hat{\theta}_{\text{UR}}$  with our orthogonal estimator  $\hat{\theta}$  in (10) in terms of the asymptotic bias and variance, respectively.

In terms of the bias, we note that  $\hat{\theta}_{\text{UR}}$  may suffer from a severe bias, because

$$\mathbb{E}(\hat{\theta}_{\text{UR}}) - \theta_0 = \{\mathbb{E}[\Phi(X)\Phi(X)^\top]\}^{-1} \mathbb{E}\{\Phi(X)[\delta_0(X) + g_0(Z)]\} + o(N^{-1/2}),$$

which can be arbitrarily large, due to both the model error  $\delta_0$  in (2), and the effect of the auxiliary modality reflected by  $g_0$  in (1). In multimodal analysis, however, both  $\delta_0$  and  $g_0$  can be substantial. Because of this bias, we have  $\sqrt{N}(\hat{\theta}_{\text{UR}} - \theta_0) = O_p(\sqrt{N})$ , which diverges as  $N$  tends to infinity. Consequently,  $\hat{\theta}_{\text{UR}}$  is unsuitable for statistical inference tasks. By contrast, the proposed orthogonal estimator  $\hat{\theta}$  is asymptotically unbiased.

In terms of the variance, we note that  $\hat{\theta}_{\text{UR}}$  achieves a variance that is no larger than that of  $\hat{\theta}$ . Specifically, the asymptotic variance of  $\hat{\theta}_{\text{UR}}$  is  $\text{Var}(\hat{\theta}_{\text{UR}}) = N^{-1}\sigma^2\{\mathbb{E}[\Phi(X)\Phi(X)^\top]\}^{-1}$ . Compared to the asymptotic variance of the orthogonal estimator  $\hat{\theta}$  as given in (11), we have,

$$\text{Var}(\hat{\theta}) - \text{Var}(\hat{\theta}_{\text{UR}}) \geq 0, \text{ as } N \rightarrow \infty,$$

in the sense that the difference of the two covariance matrices is semi-positive definite. The two asymptotic variances are equal only when  $r_0 = 0$  in (4), i.e., when the primary and auxiliary modalities are completely independent of each other. The inflated variance of  $\hat{\theta}$  compared to that of  $\hat{\theta}_{\text{UR}}$  is due to the intrinsic correlation between  $X$  and  $Z$  that is modeled by  $r_0$ . It can be viewed as a generalization of the well-known variance inflation phenomenon in the classical linear regression model due to the collinearity. For instance, consider the linear model  $Y = X\theta_0 + Z^\top\beta_0 + U$ , with  $\mathbb{E}(X) = \mathbb{E}(Y) = 0$ . The variance of the least squared estimator becomes  $\mathbb{E}(U^2)/[\mathbb{E}(X^2)(1 - \kappa)]$  after incorporating the auxiliary modality  $Z$ , where  $\kappa = \mathbb{E}(XZ^\top)[\mathbb{E}(ZZ^\top)]^{-1}\mathbb{E}(ZX)/\mathbb{E}(X^2)$  characterizes the correlation between  $X$  and  $Z$ . This variance increases compared to the case when there is no  $Z$  in the model. On the other hand, we also note that, the orthogonal estimator  $\hat{\theta}$  actually attains the smallest possible variance when  $Z$  is incorporated, as shown in Theorem 2.

## 5.2 Debiased unimodal regression

We next consider a debiased version of the unimodal regression. Numerous debiasing strategies have been successfully developed in high-dimensional regression modeling in recent years (see,

e.g., Zhang and Zhang, 2014; van de Geer et al., 2014; Cai and Guo, 2017, among others). The debiased estimator is obtained in two stages. First, the model error  $\delta_0$  is estimated based on the unimodal regression estimator  $\hat{\theta}_{\text{UR}}$  and some machine learning method as in (7),

$$\hat{\delta}_{\text{DUR}} = \arg \min_{\delta \in \mathcal{H}_\delta} \left\{ \frac{1}{N} \sum_{i=1}^N \left[ Y_i - \Phi(X_i) \hat{\theta}_{\text{UR}} - \delta(X_i) \right]^2 + \lambda_N^\delta \text{PEN}_{\mathcal{H}_\delta}(\delta) \right\},$$

where  $\lambda_N^\delta \geq 0$  is a tuning parameter. Then the debiased estimator of  $\theta_0$  is obtained by explicitly taking the model error into account,

$$\hat{\theta}_{\text{DUR}} = \arg \min_{\theta \in \mathbb{R}^d} \left\{ \frac{1}{N} \sum_{i=1}^N \left[ Y_i - \Phi(X_i)^\top \theta - \hat{\delta}_{\text{DUR}}(X_i) \right]^2 \right\}.$$

Proposition 4 characterizes the asymptotic behavior of the debiased unimodal estimator  $\hat{\theta}_{\text{DUR}}$ .

**Proposition 4.** *Suppose the conditions of Proposition 3 hold. Suppose the regularity condition (C1) holds. Then the debiased unimodal regression estimator  $\hat{\theta}_{\text{DUR}}$  satisfies that,*

$$\begin{aligned} \hat{\theta}_{\text{DUR}} - \theta_0 &= \{ \mathbb{E}[\Phi(X)\Phi(X)^\top] \}^{-1} \left\{ \frac{1}{N} \sum_{i=1}^N \Phi(X_i)[g_0(Z_i) + U_i] \right\} \\ &\quad + O_p[(\mathbb{E}\{\hat{\delta}_{\text{DUR}}(X) - \delta_0(X)\}^2)^{1/2}] + o_p(N^{-1/2}). \end{aligned}$$

The proof of the proposition is given in Supplementary Appendix. We make two observations regarding the asymptotic bias of  $\hat{\theta}_{\text{DUR}}$ . First of all,  $\hat{\theta}_{\text{DUR}}$  indeed achieves a reduced bias compared to the unimodal estimator  $\hat{\theta}_{\text{UR}}$ . This is because under the regularity condition (C3), the bias of  $\hat{\theta}_{\text{DUR}}$  is

$$\mathbb{E}(\hat{\theta}_{\text{DUR}}) - \theta_0 = \{ \mathbb{E}[\Phi(X)\Phi(X)^\top] \}^{-1} \mathbb{E}[\Phi(X)g_0(Z)] + o(N^{-1/4}).$$

Comparing this bias with that of  $\hat{\theta}_{\text{UR}}$ , we see that  $\hat{\theta}_{\text{DUR}}$  removes the bias term due to the model error  $\delta_0$  as  $N \rightarrow \infty$ , but  $\hat{\theta}_{\text{UR}}$  does not. On the other hand,  $\hat{\theta}_{\text{DUR}}$  is still an inconsistent and biased estimator of  $\theta_0$ , because  $\hat{\theta}_{\text{DUR}}$  does not remove the bias due to the effect of the auxiliary modality  $g_0$ . Consequently,  $\hat{\theta}_{\text{DUR}}$  is unsuitable for statistical inference neither.

### 5.3 Simple joint regression

Another common solution in multimodal analysis is to incorporate multiple data modalities in a simple additive fashion into a single regression model. This strategy is intuitive, and we term it as

the *simple joint regression*. Specifically, it obtains the joint estimator for  $\{\theta_0, g_0\}$  as,

$$\{\hat{\theta}_{\text{SJR}}, \hat{g}_{\text{SJR}}\} = \arg \min_{\theta \in \mathbb{R}^d, g \in \mathcal{H}_g} \left\{ \frac{1}{N} \sum_{i=1}^N [Y_i - \Phi(X_i)^\top \theta - g(Z)]^2 + \lambda_N^g \text{PEN}_{\mathcal{H}_g}(g) \right\},$$

where  $\lambda_N^g \geq 0$  is a tuning parameter, and  $\hat{g}_{\text{SJR}}$  is obtained by a machine learning method as in (7).

Proposition 5 characterizes the asymptotic behavior of the simple joint estimator  $\hat{\theta}_{\text{SJR}}$ .

**Proposition 5.** *Suppose the conditions of Proposition 3 hold. Suppose the regularity condition (C1) holds. Then the simple joint regression estimator  $\hat{\theta}_{\text{SJR}}$  satisfies that,*

$$\begin{aligned} \hat{\theta}_{\text{SJR}} - \theta_0 &= \{\mathbb{E}[\Phi(X)\Phi(X)^\top]\}^{-1} \left\{ \frac{1}{N} \sum_{i=1}^N \Phi(X_i)[\delta_0(X_i) + U_i] \right\} \\ &\quad + O_p((\mathbb{E}\{[\hat{g}_{\text{SJR}}(Z) - g_0(Z)]^2\})^{1/2}) + o_p(N^{-1/2}). \end{aligned}$$

The proof is given in Supplementary Appendix. We again study the asymptotic behavior of  $\hat{\theta}_{\text{SJR}}$ . Under the regularity condition (C3), the asymptotic bias of  $\hat{\theta}_{\text{SJR}}$  is,

$$\mathbb{E}(\hat{\theta}_{\text{SJR}}) - \theta_0 = \{\mathbb{E}[\Phi(X)\Phi(X)^\top]\}^{-1} \mathbb{E}[\Phi(X)\delta_0(X)] + o(N^{-1/4}),$$

which is not vanishing due to the non-zero model error  $\delta_0$ . The mean squared error of  $\hat{\theta}_{\text{SJR}}$  is,

$$\mathbb{E}[(\hat{\theta}_{\text{SJR}} - \theta_0)^2] = O(\mathbb{E}\{[\hat{g}_{\text{SJR}}(Z) - g_0(Z)]^2 + \delta_0^2(X)\}),$$

which does not converge at the rate of  $N^{-1}$  if  $\hat{g}_{\text{SJR}}$  is estimated using machine learning methods, or if  $\delta_0$  is not negligible. Consequently,  $\hat{\theta}_{\text{SJR}}$  is generally an inefficient and biased estimator of  $\theta_0$ .

## 5.4 Double/debiased machine learning

The recent proposal of double/debiased machine learning (DML) by Chernozhukov et al. (2018) offers an effective way for the inference of a low-dimensional parameter, such as the treatment effect or the structural parameter, in the presence of high-dimensional nuisance parameters. Our proposal is similar to DML in that both approaches employ the Neyman orthogonality and cross-fitting. However, there are two major differences. First, our method considers a flexible basis expansion type model for the parametric part of  $f_0$  for an interpretable association between the primary modality and the outcome. By contrast, DML studies a low-dimensional parameter as the primary inferential target. Second, we consider an additional model error term  $\delta_0$  in modeling

the primary function  $f_0$  in (2). Consequently, we further employ the decomposition orthogonality and residual learning when constructing the estimator  $\hat{\theta}$  to remove the bias due to  $\delta_0$ . On the other hand, DML does not consider any error term in their primary parameter of interest.

Specifically, DML randomly splits the data into  $Q$  disjoint chunks, and estimate  $g_0$  by

$$\hat{g}_{\text{DML},q} = \arg \min_{g \in \mathcal{H}_g} \left\{ \frac{1}{n} \sum_{i \in I_q^c} [Y_i - g(Z_i)]^2 + \lambda_n^g \text{PEN}_{\mathcal{H}_g}(g) \right\}.$$

where  $\lambda_n^g \geq 0$  is a tuning parameter. It then estimates  $\theta_0$  by

$$\hat{\theta}_{\text{DML}} = \left\{ \frac{1}{nQ} \sum_{q=1}^Q \sum_{i \in I_q} [\Phi(X_i) - \hat{r}_q(Z_i)] \Phi(X_i)^\top \right\}^{-1} \frac{1}{nQ} \sum_{q=1}^Q \sum_{i \in I_q} [\Phi(X_i) - \hat{r}_q(Z_i)] [Y_i - \hat{g}_{\text{DML},q}(Z_i)].$$

Proposition 6 characterizes the asymptotic behavior of DML estimator  $\hat{\theta}_{\text{DML}}$ .

**Proposition 6.** *Suppose the conditions of Proposition 3 hold. Suppose the regularity conditions (C1) to (C3) hold. Then the DML estimator  $\hat{\theta}_{\text{DML}}$  satisfies that,*

$$\hat{\theta}_{\text{DML}} - \theta_0 = (\mathbb{E}[VV^\top])^{-1} \left( \frac{1}{N} \sum_{i=1}^N V_i U_i \right) + O_p(\{\mathbb{E}[\delta_0^2(X)]\}^{1/2}) + o_p(N^{-1/2}).$$

The proof is given in Supplementary Appendix. The mean squared error of  $\hat{\theta}_{\text{DML}}$  is,

$$\mathbb{E}[(\hat{\theta}_{\text{DML}} - \theta_0)^2] = \frac{1}{N} \sigma^2 (\mathbb{E}[VV^\top])^{-1} + O(\mathbb{E}[\delta_0^2(X)]) + o(N^{-1}).$$

Compared to our estimator  $\hat{\theta}$ , whose mean squared error is  $N^{-1} \sigma^2 (\mathbb{E}[VV^\top])^{-1} + o(N^{-1})$ ,  $\hat{\theta}_{\text{DML}}$  has an inflated mean squared error at the order of  $\mathbb{E}[\delta_0^2(X)]$ . Consequently, it cannot achieve the  $\sqrt{N}$ -consistency if the model error  $\delta_0$  is not negligible.

## 6 Simulations

We next study the finite-sample performance of the proposed Orthogonal STatistical INference method (abbreviated as OSTIN). We consider three synthetic examples. The first example evaluates the performance of inferring  $\theta_0$  in an additive model setting. We also numerically compare with the alternative methods of unimodal regression (UR), debiased unimodal regression (DUR), simple joint regression (SJR), and double machine learning (DML). The second example studies

the sensitivity of using different machine learning methods for nuisance function estimation in a more complicated model with interactions. We compare with SJR and DML, but exclude UR and DUR since they do not involve any nuisance function estimation. The last example evaluates the performance of inferring  $f_0$  in a high-dimensional additive setting. In all these examples, the model error  $\delta_0$  is estimated in the RKHS constructed as in Proposition 2. We use the Matérn kernel  $K(x, x') = (1 + \sqrt{5}\|x - x'\| + 5\|x - x'\|^2/3) \exp(-\sqrt{5}\|x - x'\|)$ , where the corresponding RKHS contains twice differentiable functions (Gneiting et al., 2010). The tuning parameter  $\lambda_n^\delta$  in (7) is selected by generalized cross-validation (Wahba, 1990). We set  $Q = 2$  in Algorithm 1.

## 6.1 Empirical performance of $\theta_0$ inference

We begin with an additive model,  $Y_i = f_0(X_i) + g_{01}(Z_{i1}) + g_{02}(Z_{i2}) + g_{03}(Z_{i3}) + U_i$ , where

$$\begin{aligned} f_0(x) &= 5x - [\cos(2\pi x) + \sin(2\pi x)], \\ g_{01}(z_1) &= 6[0.1 \sin(2\pi z_1) + 0.2 \cos(2\pi z_1) + 0.3 \sin^2(2\pi z_1) + 0.4 \cos^3(2\pi z_1) + 0.5 \sin^3(2\pi z_1)], \\ g_{02}(z_2) &= 3(2z_2 - 1)^2, \quad g_{03}(z_3) = \frac{4 \sin(2\pi z_3)}{2 - \sin(2\pi z_3)}. \end{aligned}$$

We generate random variables  $E_1, \dots, E_5$  independently from Uniform $[0, 1]$ , and set the primary and auxiliary modalities as  $X = (E_1 + \rho E_5)/(1 + \rho) \in \mathcal{X} = [0, 1]$ , and  $Z_j = (E_{j+1} + \rho E_5)/(1 + \rho)$ , for some  $\rho > 0$  and  $j = 1, 2, 3$ . The correlation between any two variables in  $X$  and  $Z$  is thus  $\rho^2/(1 + \rho^2)$ . We generate i.i.d. copies  $(X_i, Z_{i1}, Z_{i2}, Z_{i3})$  of  $(X, Z_1, Z_2, Z_3)$ , and generate the error  $U_i$  from  $\mathcal{N}(0, \sigma^2)$ . We set the sample size  $N = 500$ . We set  $\eta(x, \theta_0) = \theta_0 x$ , and apply the random forests averaged over 500 trees to estimate the nuisance functions  $\{r_0, g_0\}$ .

Figure 1 shows the histograms of the competing estimators,  $\hat{\theta}_{\text{UR}}, \hat{\theta}_{\text{DUR}}, \hat{\theta}_{\text{SJR}}, \hat{\theta}_{\text{DML}}$ , and our orthogonal estimator  $\hat{\theta}$ , under  $\rho = 1$  and  $\sigma = 1$ , based on 500 data replications. It is clearly seen that the four competing estimators are biased, whereas the histogram of the orthogonal estimator matches that of the normal distribution. Figure 2 further reports the empirical mean squared error of different estimators under various combinations of the noise level  $\sigma$  and the correlation level  $\rho$ . When  $\sigma^{-1}$  increases, the signal-to-noise ratio increases. However, the mean squared errors of the four competing methods do not decrease much due to the estimation bias, whereas the mean squared error of our orthogonal estimator continuously decreases.

## 6.2 Sensitivity of nuisance function modeling for $\theta_0$ inference

We next consider a complex nonlinear model with interactions,  $Y_i = f_0(X_i) + h_{01}(Z_{i1})g_{02}(Z_{i2}) + h_{02}(Z_{i1})g_{03}(Z_{i3}) + h_{03}(Z_{i3})g_{04}(Z_{i4}) + U_i$ , where

$$\begin{aligned} f_0(x) &= -2 \sin(2\pi x) + 5(1 - e^x)^2; \\ h_{01}(z_1) &= \frac{15}{8} [1 - (4z_1 - 1)^2]^2, \quad h_{02}(z_1) = 3 \cos(2\pi z_1), \quad h_{03}(z_1) = 4; \\ g_{02}(z_z) &= z_z^2 - \frac{1}{3}, \quad g_{03}(z_3) = z_3 - \frac{1}{2}, \quad g_{04}(z_4) = e^{z_4} + e^{-1} - 1. \end{aligned}$$

A similar model has been considered in Lu et al. (2020). We generate random variables  $E_1, \dots, E_6$  independently from  $\text{Uniform}[0, 1]$ , and set the primary and auxiliary modalities as  $X = (E_1 + \rho E_6)/(1 + \rho)$ , and  $Z_j = (E_{j+1} + \rho E_6)/(1 + \rho)$ , for  $\rho = 1$  and  $j = 1, \dots, 4$ . We generate i.i.d. copies  $(X_i, Z_{i1}, Z_{i2}, Z_{i3}, Z_{i4})$  of  $(X, Z_1, Z_2, Z_3, Z_4)$ , and generate the error  $U_i$  from  $\mathcal{N}(0, \sigma^2)$  with  $\sigma = 1$ . We set the sample size  $N \in \{400, 500, 600\}$ . We set  $\eta(x, \theta_0) = \theta_0 \sin(2\pi x)$ .

We apply a number of different nonlinear machine learning methods to estimate the nuisance functions  $\{r_0, g_0\}$ , including random forests, boosted trees, and neural networks. For boosted trees, we tune the regularization parameters by ten-fold cross-validation. For neural networks, we use five hidden layers with ten neuron at each hidden layer, and choose the learning rate of 0.02

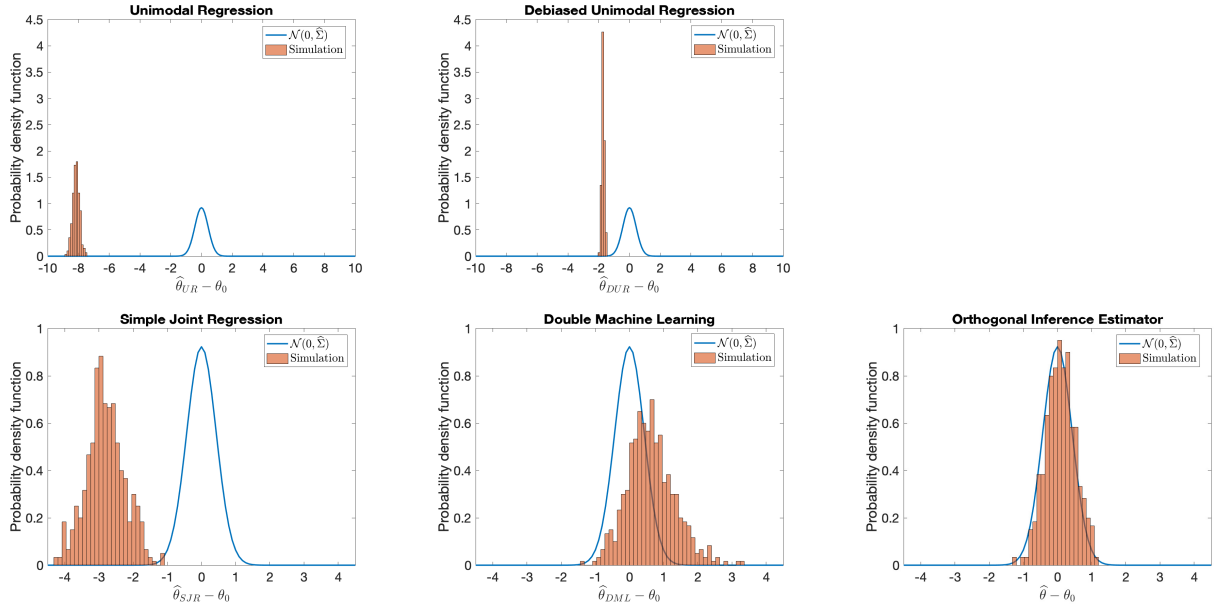


Figure 1: Empirical distribution of the estimator of  $\theta_0$  based on 500 data replications. The bell-shape curve denotes the oracle normal distribution.

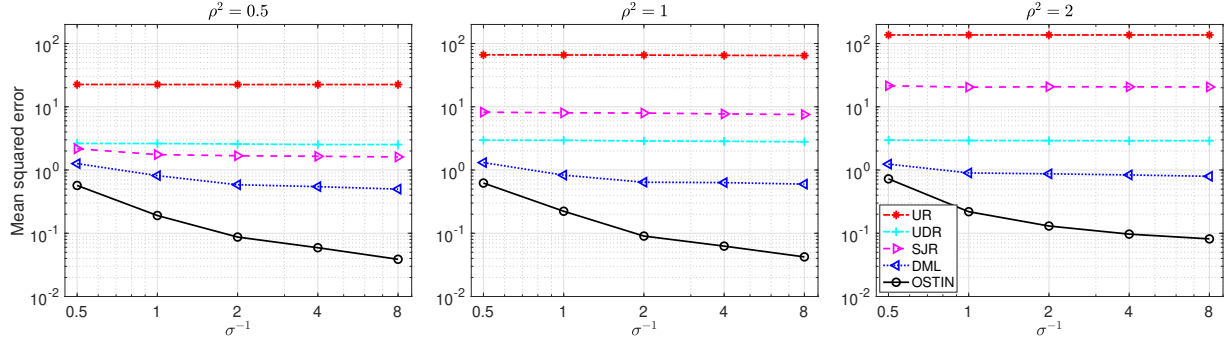


Figure 2: Mean squared error of the estimator of  $\theta_0$  with varying noise level  $\sigma$  and correlation level  $\rho$ . Both axes are in the log scale.

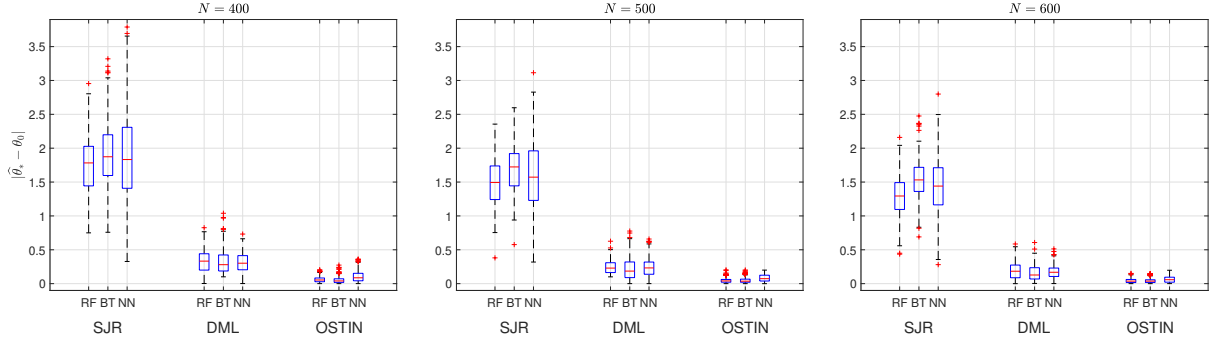


Figure 3: Absolute error of the estimation of  $\theta_0$ , with varying sample size and different machine learning methods, including random forests (RF), boosted trees (BT), and neural networks (NN).

and a linear activation function.

Figure 3 reports the absolute error of estimating  $\theta_0$  under various combinations of the sample size  $N$  and the nonlinear modeling methods, based on 500 data replications. It is seen that our orthogonal estimator achieves the smallest bias and standard deviation, and the results are relatively stable across different choices of the nonlinear modeling methods for the nuisance functions.

### 6.3 Empirical performance of $f_0$ inference

We next consider a high-dimensional additive model,  $Y_i = f_0(X_i) + \sum_{j=1}^{600} g_{0j}(Z_{ij}) + U_i$ , where  $f_0(x), g_{01}(z_1), g_{02}(z_2), g_{03}(z_3)$  are the same as the first example, and

$$g_{0j}(z_j) = z_j, \text{ for } j \in \{4, \dots, 100\}, \quad g_{0j}(z_j) = 0, \text{ for } j \in \{101, \dots, 600\}.$$



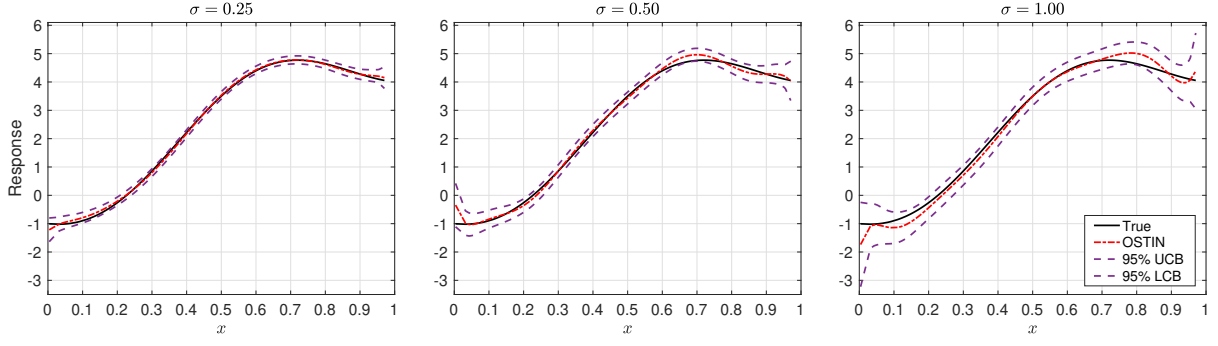


Figure 4: The true and estimated primary function  $f_0(x)$ , with the 95% upper and lower confidence bounds, of the orthogonal method, under varying noise level  $\sigma$ .

We generate random variables  $E_1, \dots, E_{602}$  independently from  $\text{Uniform}[0, 1]$ , and set the primary and auxiliary modalities as  $X = (E_1 + \rho E_{602}) / (1 + \rho)$ , and  $Z_j = (E_{j+1} + \rho E_{602}) / (1 + \rho)$ , for  $\rho = 1$  and  $j = 1, \dots, 600$ . We generate i.i.d. copies  $(X_i, Z_{i1}, Z_{i2}, \dots, Z_{i600})$  of  $(X, Z_1, Z_2, \dots, Z_{600})$ , and generate the error  $U_i$  from  $\mathcal{N}(0, \sigma^2)$  with  $\sigma \in \{0.25, 0.5, 1\}$ . We set the sample size  $N = 500$ .

We construct both the confidence band (12) for the primary effect  $f_0(x)$ , and the confidence interval (13) for the coefficient of determination  $R^2$ . We use polynomial basis functions with  $s = 5$  following Theorem 3, while we estimate  $\delta_0$  in a similar way as in the first example. We employ the Lasso to estimate the nuisance functions  $\{r_0, g_0\}$  due to the high-dimensionality of this example, and tune the Lasso parameter using tenfold cross-validation. We compute the quantile estimator  $\hat{c}_N(\alpha/2)$  in (12) by bootstrap with 500 replications.

Figure 4 shows the true and estimated primary function  $f_0(x)$ , along with the 95% upper and lower confidence bounds, of the proposed orthogonal method with the varying noise level  $\sigma$ . We also compute the empirical coverage probability of  $\text{CI}(f_0(x))$  at the significance level 95%, by discretizing the interval  $\mathcal{X} = [0, 1]$  into 1000 grids, then calculating the percentage that the confidence band covers the truth on the 1000 grid points in 500 data replications. The resulting coverage probability is 0.968, 0.958 and 0.946, when  $\sigma = 0.25, 0.50$  and 1.00, respectively. Moreover, we compute the empirical coverage probability of  $\text{CI}(R^2)$  as the percentage that the confidence interval covers the true  $R^2$ . The resulting coverage probability is 0.990, 0.972 and 0.964, when  $\sigma = 0.25, 0.50$  and 1.00, respectively. It is seen from both the estimated function and the coverage probability that our proposed orthogonal method works well.

## 7 Multimodal Neuroimaging Study for Alzheimer’s Disease

We revisit the motivating example of multimodal neuroimaging analysis for Alzheimer’s disease. The data is part of the Berkeley Aging Cohort Study, and consists of 697 subjects. For each subject, the imaging data includes the anatomical MRI scan, which measures brain cortical thickness and is summarized as a 68-dimensional vector that corresponds to 68 predefined brain regions-of-interest (ROIs), and the PET scan, which measures tau deposition and is summarized as a 70-dimensional vector that corresponds to 70 ROIs. In addition, the subject’s age, gender, education, and a scalar measure of the total amyloid- $\beta$  accumulation are collected. The response is a composite cognition score that combines assessments of episodic memory, timed executive function, and global cognition. We study two scientific questions given this data, first, the effect of brain atrophy on cognition after controlling for demographic variables and amyloid- $\beta$ , tau depositions, and second, the cascade of AD biomarkers as suggested by Jack et al. (2010, 2013).

For the first problem, we take the brain MRI cortical thickness as the primary modality, with  $p = 68$ , and take the PET tau deposition along with the demographic variables and the total amyloid- $\beta$  as the auxiliary modalities, resulting in  $p' = 74$ . We apply the proposed method to infer the effect of cortical thickness of individual brain regions on the cognitive outcome. We adopt a similar implementation as used in our first simulation example, and set  $\eta(x, \theta_0) = \theta_0^\top x$ . Table 1 reports the orthogonal estimate of the effects of the brain regions where the cortical thickness is found to be significantly correlated with the cognitive outcome after controlling for amyloid- $\beta$ , tau and other covariates, with the corresponding  $p$ -values under the FDR control at the 5% level (Benjamini and Hochberg, 1995). These findings agree well with the AD literature. Particularly,

Table 1: Multimodal study of AD: the identified significant brain regions.

	Estimate	SD	$p$ -value
Entorhinal cortex, left	3.214	0.709	$6.957 \times 10^{-6}$
Entorhinal cortex, right	2.853	0.671	$2.454 \times 10^{-5}$
Superior temporal cortex, left	10.42	2.444	$2.321 \times 10^{-5}$
Superior temporal cortex, right	5.061	1.451	$5.213 \times 10^{-4}$
Parahippocampal gyrus, left	1.076	0.362	$3.112 \times 10^{-3}$
Parahippocampal gyrus, right	1.366	0.474	$4.098 \times 10^{-3}$

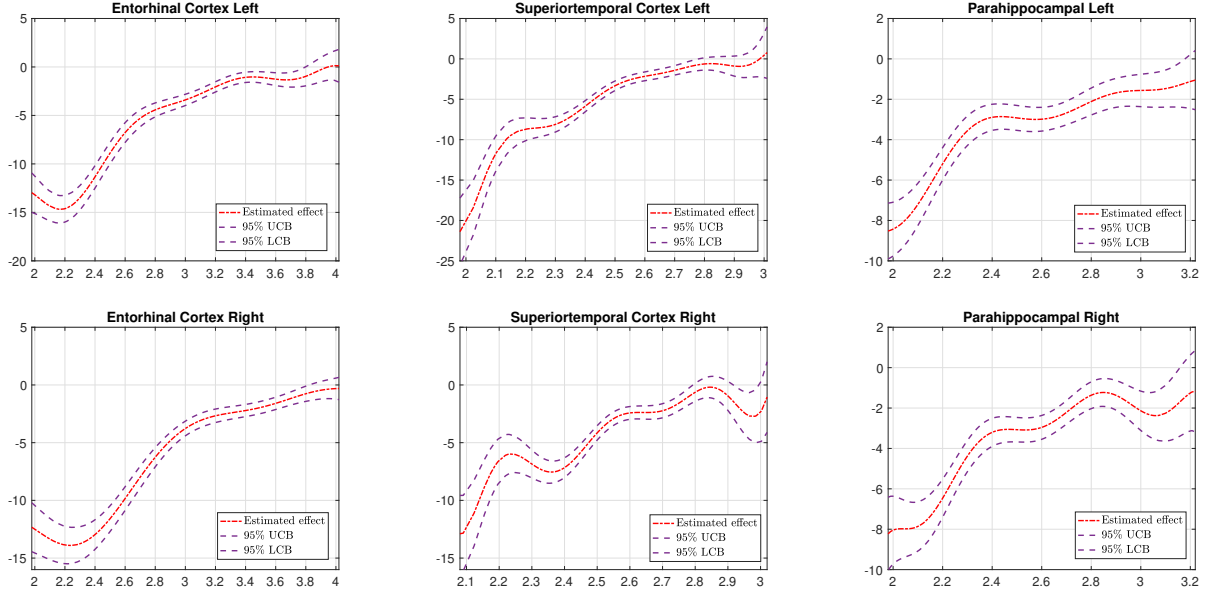


Figure 5: The estimated individual effect of the significant brain regions.

the entorhinal cortex is a brain area located in the medial temporal lobe, and functions as a hub in a widespread network for memory, navigation and the perception of time. Atrophy in the entorhinal cortex has been consistently reported in AD (Pini et al., 2016). The parahippocampal gyrus is a grey matter cortical region of the brain that surrounds the hippocampus, and plays an important role in memory encoding and retrieval. It is among the first to suffer damage from AD (Jack et al., 2011). The superior temporal gyrus locates in the temporal lobe, and contains the Wernicke's area responsible for processing of speech. Its connection with AD needs further verification. Moreover, Figure 5 shows the confidence band for the estimated individual effect of each significant brain region. Besides, the 95% confidence interval for the  $R^2$  measure is (0.402, 0.437), which supports the common belief that brain structural atrophy is closely related to the cognition outcome.

For the second problem, Jack et al. (2010, 2013) suggested that tau deposition precedes structural atrophy in AD pathogenesis. To help verify this theory, we take the PET tau deposition as the primary modality, with  $p = 70$ , then compare two model fits, one with the MRI cortical thickness as part of the auxiliary modalities, and the other without. In both models, we include age, gender, education and amyloid- $\beta$  as the auxiliary modalities. This yields  $p' = 72$  when the cortical thickness is included, and  $p' = 4$  if not. We obtain the 95% confidence interval for the total effect of tau, which is  $(-1.724, 0.702)$  when the cortical thickness is included, and  $(-5.212, -3.945)$

when it is not. These results suggest that, not including the brain structural atrophy as the auxiliary modality would result in a much larger effect of tau on cognition outcome, which in turn implies that brain structural atrophy likely occurs after tau deposition. As such, it lends some support to the theory of Jack et al. (2010, 2013).

## References

- Alam, M. A., Lin, H.-Y., Deng, H.-W., Calhoun, V. D., and Wang, Y.-P. (2018). A kernel machine method for detecting higher order interactions in multimodal datasets: Application to schizophrenia. *Journal of Neuroscience Methods*, 309:161–174.
- Baltrusaitis, T., Ahuja, C., and Morency, L.-P. (2019). Multimodal machine learning: A survey and taxonomy. *IEEE Transactions on Pattern Analysis and Machine Intelligence*, 41(2):423–443.
- Benjamini, Y. and Hochberg, Y. (1995). Controlling the false discovery rate: a practical and powerful approach to multiple testing. *Journal of the Royal Statistical Society, Series B.*, 57(1):289–300.
- Biau, G. (2012). Analysis of a random forests model. *Journal of Machine Learning Research*, 13(1):1063–1095.
- Bickel, P. J., Ritov, Y., and Tsybakov, A. B. (2009). Simultaneous analysis of lasso and dantzig selector. *The Annals of statistics*, 37(4):1705–1732.
- Breiman, L. (2001). Statistical modeling: The two cultures. *Statistical Science*, 16(3):199–231.
- Bühlmann, P. and van de Geer, S. (2011). *Statistics for High-Dimensional Data: Methods, Theory and Applications*. Springer Science & Business Media.
- Buja, A., Hastie, T., and Tibshirani, R. (1989). Linear smoothers and additive models. *The Annals of Statistics*, 17(2):453–510.
- Cai, Q., Wang, H., Li, Z., and Liu, X. (2019). A survey on multimodal data-driven smart healthcare systems: Approaches and applications. *IEEE Access*, 7:133583–133599.
- Cai, T. T. and Guo, Z. (2017). Confidence intervals for high-dimensional linear regression: Minimax rates and adaptivity. *The Annals of Statistics*, 45(2):615–646.
- Chen, X. and White, H. (1999). Improved rates and asymptotic normality for nonparametric neural network estimators. *IEEE Transactions on Information Theory*, 45(2):682–691.

- Chernozhukov, V., Chetverikov, D., Demirer, M., Duflo, E., Hansen, C., Newey, W., and Robins, J. (2018). Double/debiased machine learning for treatment and structural parameters: Double/debiased machine learning. *The Econometrics Journal*, 21:C1–C68.
- Chernozhukov, V., Chetverikov, D., and Kato, K. (2014). Anti-concentration and honest, adaptive confidence bands. *The Annals of Statistics*, 42(5):1787–1818.
- Fan, J. and Lv, J. (2008). Sure independence screening for ultrahigh dimensional feature space. *Journal of the Royal Statistical Society, Series B.*, 70(5):849–911.
- Friedman, J. H. (2001). Greedy function approximation: a gradient boosting machine. *The Annals of Statistics*, 29(5):1189–1232.
- Gneiting, T., Kleiber, W., and Schlather, M. (2010). Matérn cross-covariance functions for multivariate random fields. *Journal of the American Statistical Association*, 105(491):1167–1177.
- Hastie, T. and Tibshirani, R. (1990). *Generalized Additive Models*. CRC Press.
- Hinrichs, C., Singh, V., Xu, G., Johnson, S. C., and Initiative, A. D. N. (2011). Predictive markers for ad in a multi-modality framework: an analysis of mci progression in the adni population. *Neuroimage*, 55(2):574–589.
- Huang, J. Z., Zhang, L., and Zhou, L. (2007). Efficient estimation in marginal partially linear models for longitudinal/clustered data using splines. *Scandinavian Journal of Statistics*, 34(3):451–477.
- Jack, C. R., Barkhof, F., Bernstein, M. A., et al. (2011). Steps to standardization and validation of hippocampal volumetry as a biomarker in clinical trials and diagnostic criterion for alzheimer’s disease. *Alzheimer’s & Dementia*, 7(4):474–485.e4.
- Jack, C. R., Knopman, D. S., Jagust, W. J., Shaw, L. M., Aisen, P. S., Weiner, M. W., Petersen, R. C., and Trojanowski, J. Q. (2010). Hypothetical model of dynamic biomarkers of the alzheimer’s pathological cascade. *The Lancet Neurology*, 9(1):119 – 128.
- Jack, Clifford R, J., Knopman, D. S., Jagust, W. J., Petersen, R. C., Weiner, M. W., Aisen, P. S., Shaw, L. M., Vemuri, P., Wiste, H. J., Weigand, S. D., Lesnick, T. G., Pankratz, V. S., Donohue, M. C., and Trojanowski, J. Q. (2013). Tracking pathophysiological processes in alzheimer’s disease: an updated hypothetical model of dynamic biomarkers. *The Lancet. Neurology*, 12(2):207–216.
- Kosorok, M. R. (2007). *Introduction to Empirical Processes and Semiparametric Inference*. Springer Science & Business Media, New York.

- Kozbur, D. (2020). Inference in additively separable models with a high-dimensional set of conditioning variables. *Journal of Business & Economic Statistics*, pages 1–17.
- Li, G., Liu, X., and Chen, K. (2019). Integrative multi-view reduced-rank regression: Bridging group-sparse and low-rank models. *Biometrics*, 75(2):593–602.
- Li, Q. and Li, L. (2020). Integrative factor regression and its inference for multimodal data analysis. *arXiv preprint*, page arXiv:1911.04056.
- Lin, Y. and Zhang, H. H. (2006). Component selection and smoothing in multivariate nonparametric regression. *The Annals of Statistics*, 34(5):2272–2297.
- Lock, E. F., Hoadley, K. A., Marron, J. S., and Nobel, A. B. (2013). Joint and individual variation explained (jive) for integrated analysis of multiple data types. *The Annals of Applied Statistics*, 7(1):523.
- Lowe, R., Wu, Y., Tamar, A., Harb, J., Abbeel, P., and Mordatch, I. (2017). Multi-agent actor-critic for mixed cooperative-competitive environments. In *Proceedings of the 31st International Conference on Neural Information Processing Systems*, pages 6382–6393. Curran Associates.
- Lu, J., Kolar, M., and Liu, H. (2020). Kernel meets sieve: Post-regularization confidence bands for sparse additive model. *Journal of the American Statistical Association*, pages 1–16.
- Ma, S., Carroll, R. J., Liang, H., and Xu, S. (2015). Estimation and inference in generalized additive coefficient models for nonlinear interactions with high-dimensional covariates. *Annals of Statistics*, 43(5):2102.
- Mai, Q. and Zhang, X. (2019). An iterative penalized least squares approach to sparse canonical correlation analysis. *Biometrics*, 75(3):734–744.
- Nathoo, F. S., Kong, L., Zhu, H., and for the Alzheimer’s Disease Neuroimaging Initiative (2019). A review of statistical methods in imaging genetics. *Canadian Journal of Statistics*, 47(1):108–131.
- Newey, W. K. (1990). Semiparametric efficiency bounds. *Journal of Applied Econometrics*, 5(2):99–135.
- Newey, W. K. and Robins, J. R. (2018). Cross-fitting and fast remainder rates for semiparametric estimation. *arXiv preprint arXiv:1801.09138*.
- Neyman, J. (1959). Optimal asymptotic tests of composite statistical hypotheses. In U. Grenander (Ed.), *Probability and Statistics*, pages 416–444.

- Neyman, J. (1979).  $c(\alpha)$  tests and their use. *Sankhya*, pages 1–21.
- Pearl, J. (2009). *Causality*. Cambridge University Press, Cambridge.
- Pini, L., Pievani, M., Bocchetta, M., Altomare, D., Bosco, P., Cavedo, E., Galluzzi, S., Marizzoni, M., and Frisoni, G. B. (2016). Brain atrophy in alzheimer’s disease and aging. *Ageing Research Reviews*, 30:25–48. Brain Imaging and Aging.
- Raskutti, G., Wainwright, M. J., and Yu, B. (2011). Minimax rates of estimation for high-dimensional linear regression over  $\ell_q$ -balls. *IEEE Transactions on Information Theory*, 57(10):6976–6994.
- Richardson, S., Tseng, G. C., and Sun, W. (2016). Statistical methods in integrative genomics. *Annual Reviews of Statistics and Its Applications*, 3:181–209.
- Robins, J. M. and Rotnitzky, A. (1995). Semiparametric efficiency in multivariate regression models with missing data. *Journal of the American Statistical Association*, 90(429):122–129.
- Shu, H., Wang, X., and Zhu, H. (2020). D-cca: A decomposition-based canonical correlation analysis for high-dimensional datasets. *Journal of the American Statistical Association*, 115(529):292–306.
- Sperling, R. A., Mormino, E. C., Schultz, A. P., et al. (2019). The impact of amyloid-beta and tau on prospective cognitive decline in older individuals. *Annals of Neurology*, 85(2):181–193.
- Uludağ, K. and Roebroeck, A. (2014). General overview on the merits of multimodal neuroimaging data fusion. *Neuroimage*, 102:3–10.
- van de Geer, S., Bühlmann, P., Ritov, Y. A., and Dezeure, R. (2014). On asymptotically optimal confidence regions and tests for high-dimensional models. *The Annals of Statistics*, 42(3):1166–1202.
- van der Vaart, A. W. (1998). *Asymptotic Statistics*. Cambridge Series in Statistical and Probabilistic Mathematics. Cambridge University Press, Cambridge.
- Wahba, G. (1990). *Spline Models for Observational Data*. SIAM, Philadelphia.
- Wang, L., Xue, L., Qu, A., and Liang, H. (2014). Estimation and model selection in generalized additive partial linear models for correlated data with diverging number of covariates. *The Annals of Statistics*, 42(2):592–624.
- Xue, F. and Qu, A. (2020). Integrating multi-source block-wise missing data in model selection. *Journal of the American Statistical Association*, accepted.

- Zhang, C. and Zhang, S. (2014). Confidence intervals for low dimensional parameters in high dimensional linear models. *Journal of the Royal Statistical Society. Series B.*, 76(1):217–242.
- Zhao, Q. and Hastie, T. (2021). Causal interpretations of black-box models. *Journal of Business & Economic Statistics*, 39(1):272–281.
- Zhu, H., Khondker, Z., Lu, Z., and Ibrahim, J. G. (2014). Bayesian Generalized Low Rank Regression Models for Neuroimaging Phenotypes and Genetic Markers. *Journal of the American Statistical Association*, 109(507):977–990.